

EFFECTS OF FACE PLATES AND EDGE STRIPS ON HYDROSTATIC PIEZOELECTRIC RESPONSE OF 1-3 COMPOSITES

J. ZHAO, Q. M. ZHANG† and WENWU CAO

*Intercollege Materials Research Laboratory, The Pennsylvania State University,
University Park, PA 16802, U.S.A.*

(Received May 2, 1995)

Piezoceramic-polymer composites with 1-3 connectivity provide higher hydrostatic figure of merit $d_h g_h$ and low density, which make them attractive for underwater applications. By incorporating rigid face plates on the composite electrode surfaces, the transverse piezoelectric response can be reduced effectively and d_h increased significantly. When edge strips are put on the lateral dimensions, the hydrostatic response of the composite may be further improved, depending on the ratio of the sample thickness to the sample lateral dimensions and the elastic properties of the edge strips. In this work the effects of the rigid face plates and the edge strips on the piezoelectric response of 1-3 composites with different lateral dimensions were investigated. All the experimental features can be well accounted for by using the shear-coupling model developed recently by us and the isostrain model. Based on these results the relationship between the d_h of the face plated 1-3 composite and the elastic properties of the polymer matrix as well as other design parameters is derived, which can serve as a guideline to optimize the material selection for 1-3 composites with larger hydrostatic response.

Keywords: Piezocomposite, hydrostatic piezoelectricity, mechanical properties.

I. INTRODUCTION

Piezoelectric ceramic-polymer composites with 1-3 connectivity possess many promising features which make them attractive for hydrostatic applications.¹⁻⁵ As has been demonstrated, both theoretically and experimentally, with a small aspect ratio of the ceramic rods and a proper ceramic content, the piezoelectric hydrostatic figure of merit $d_h g_h$ (d_h and g_h are the piezoelectric hydrostatic charge and voltage coefficients respectively) of a composite can be substantially higher than the constituent ceramic phase.^{2,6} However, to fully utilize the potential of a 1-3 composite for hydrostatic applications, several issues have to be addressed. Small aspect ratio of ceramic rods will incur a high manufacturing cost and low reliability of the rods. The Poisson's ratio effect, which reduces the effect pressure on the polymer matrix in the ceramic rod poling direction by a factor of $(1 - 2\sigma)$ where σ is the Poisson's ratio of the polymer phase, drastically cuts down the effectiveness of the stress transfer from the polymer to the ceramic rods.⁷ In the past, a great deal of effort have been devoted to address these issues and some progress has been made. One of the effective ways to improve the hydrostatic response of a 1-3 composite is to glue rigid face plates on the two electrode surfaces, as schematically drawn in Figure 1(a). Throughout this paper, the following convention will be used: the 3-direction (or the z-direction) is along the ceramic rod axial (poling) direction, the 1 and 2-directions (or x and y-directions) are in the plane perpendicular to the poling directions.

†Author to whom all correspondence should be addressed.

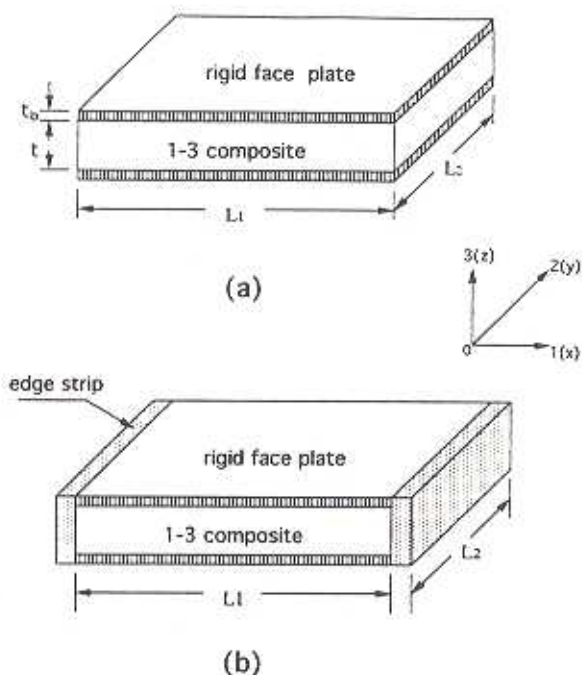


FIGURE 1 (a) Schematic drawing of a face plated 1-3 composite, (b) schematic drawing of a face plated 1-3 composite with edge strips at two end faces in the 1-direction.

The effect of rigid face plates on a 1-3 piezocomposite can be summarized as follows: (1) it improves the stress transfer between the ceramic rods and polymer matrix in the ceramic poling direction so that the composite approaches the isostrain situation; (2) it improves the bonding between the ceramic rods and polymer matrix; (3) it reduces Poisson's ratio effect and the d_{31} effect. The effect (1) has been investigated and the results have been reported in another publication.⁸ The reason for effect (2) is quite obvious. In this paper, the results of a recent investigation on effect (3) will be presented and in all the discussion, the stress transfer in the 3-direction is assumed to be that of isostrain results due to the face plates.

When rigid face plates are glued onto the two faces of a 1-3 composite, due to the fact that the elastic stiffness of the plates is much higher than that of the composite in the lateral dimensions, most of the pressure in these directions will be born by the face plates, which reduces the effective d_{31} and d_{32} coefficients of the whole sample and increases d_h since $d_h = d_{33} + d_{31} + d_{32}$. In addition to that, the much reduced lateral pressure on the polymer matrix greatly reduces the Poisson's ratio effect.

Based on an earlier work by Wang *et al.*⁹ to treat the clamping effect of the face plates on 1-3 composites and the isostrain model^{2,3,5} to calculate the effective material properties of the composite, a theoretical treatment will be presented in this paper, which quantitatively analyzes how various parameters affect these two effects and provides a general guideline to the design of a face plated 1-3 composite.

For a face plated 1-3 composite, as shown schematically in Figure 1(a), the clamping effect of the face plates in the lateral dimensions is through shear force, a situ-

ation quite similar to a 2-2 composite. As has been demonstrated earlier,^{2,10} the effectiveness of this clamping effect will depend on the sample dimension, especially, the ratio of the 1-3 composite thickness t to its lateral dimension L . To evaluate this dimensional effect, experiments were carried out systematically on 1-3 composites with different ratio of t/L . The results are in excellent agreement with the theoretical calculation based on the shear coupling model.¹⁰

To improve the stress transfer in the lateral directions between the face plates and 1-3 composite, one can put edge strips on the end faces of the face plated 1-3 composite, as schematically drawn in Figure 1(b). The effect of the edge strips on the hydrostatic response of 1-3 composite with different dimensions was also investigated and will be reported in the paper.

II. EXPERIMENTS

Two 1-3 composites with 15% volume content ceramic rods and different polymer matrix were made and tested. The polymer matrix for the first composite (labeled as composite I) is Spurr's epoxy and the second one (labeled as composite II) is polyurethane mixed with 50% volume of microballon of about 20 μm size. As listed in Table I, the two have quite different elastic properties.¹¹ The ceramic rods of lead zirconate titanate (PZT) used for the two composites were manufactured by CPSS Co. (MA). The composition of the rods is similar to that of PZT-5H and the diameter of the rods is 1.10 mm. The piezoelectric and dielectric properties of the PZT rods used for the two composites are also listed in Table I. Both composites were poled at a poling voltage of 25 kV/cm at room temperature for three minutes.

The initial dimensions of the composite with Spurr's epoxy matrix are: $t = 5.62$ mm, $L_2 = 27$ mm, and $L_1 = 38.5$ mm. Brass plates with thickness $t = 0.79$ mm were used as the face plates and J-B weld cement of J-B weld Co. was used to glue the brass plates to the composite. Glass reinforced polymer (GRP) plate ($t = 1.6$ mm) and alumina plate ($t = 3.5$ mm) were tested for edge strip materials. The bonding between the edge strip and face plated 1-3 composite was provided by a 5 minute epoxy of Devcon Corporation.

The initial dimensions of the composite with polyurethane mixed with 50% microballon matrix are: $t = 5.54$ mm, $L_2 = 35$ mm, and $L_1 = 52.5$ mm. Since the elastic stiffness of the polymer matrix here is much lower than that of spurr's epoxy, a GRP plate ($t = 1.6$ mm) was used for the face plates. Silver epoxy (Insulating Materials Inc.) was used to glue the face plates and 1-3 composite together. For this structure, only alumina plates ($t = 3.5$ mm) were used as edge strips. The elastic properties of the face plate materials as well as the plates thickness are summarized in Table II.¹²

The effective dielectric constant ϵ , the piezoelectric hydrostatic charge coefficient

TABLE I
Some properties of the polymer matrix and PZT rods for the two composites

	s_{11}^0 (m^2/N)	σ^0	d_{33} (pC/N)	d_{31} (pC/N)	ϵ
Composite I	2×10^{-10}	0.36	450	-208	2333
Composite II	5×10^{-8}	0.36	481	-222	2533

TABLE II
Properties of face plates

	t (mm)	s_{11} (m ² /N)	s_{12}
GRP	1.6	$2.63 \cdot 10^{-11}$	$-0.789 \cdot 10^{-11}$
Brass	0.79	$0.97 \cdot 10^{-11}$	$-0.32 \cdot 10^{-11}$

d_h , piezoelectric d_{33} coefficients were evaluated for these composites. Surface profile scans using a double beam laser dilatometer were also made to characterize the nonuniform strain distribution in the face plated 1-3 composites.¹³ The dielectric constant was measured using a HP multi-frequency RLC meter (HP 4192A). The d_h was measured by a comparison method where the test sample and a standard sample with known d_h value are subjected to the same quasi-static pressure (50 Hz) and the charge outputs from the two samples were compared. d_{33} coefficient of the samples was measured using both a Berlincourt d_{33} meter and a laser dilatometer. The effective d_{33} coefficient of the composites was evaluated using a laser dilatometer and will be discussed in detail later in the text. The dimensional effect of face plated 1-3 composites was investigated by reducing the sample length L_1 while keeping L_2 constant. All the relevant material parameters were evaluated for samples with different L_1 .

To distinguish the hydrostatic charge coefficient d_h measured for a 1-3 composite without face plates and with face plates, d_h and d'_h are used corresponding to the two situations. The same convention will also be used for the other parameters when needed.

III. EXPERIMENTAL RESULTS FOR COMPOSITE I

Shown in Figure 2 is d'_h of face plated 1-3 composite with Spurr's epoxy matrix measured at different L_1 . For comparison, d_h of the composite without face plates was also measured and it is 43 pC/N. Clearly, without face plates, d_h of the composite is not any better than the ceramic rods even though its d_{hg} value is improved owing to the smaller effective dielectric constant of the composite. Face plates significantly increase the hydrostatic piezoelectric response of a composite. Figure 2 also shows that d'_h decreases drastically with decreasing L_1 , which is caused by the incomplete clamping of the face plates on the 1-3 composite for samples with large t/L ratio.

If the composite is effectively clamped in the lateral dimensions by the face plates, it is expected that the whole sample will exhibit very small d_{31} and d_{32} coefficients. Figure 3(a) shows the lateral strain profiles, measured by the double beam laser dilatometer, in the 1-direction of face plated composite for different L_1 while L_2 was kept constant and the samples were driven with an electric field of 1 V/m. These surface profiles are quite similar to those of 2-2 composites measured earlier, which is consistent with the fact that a 1-3 composite with face plates can be viewed as

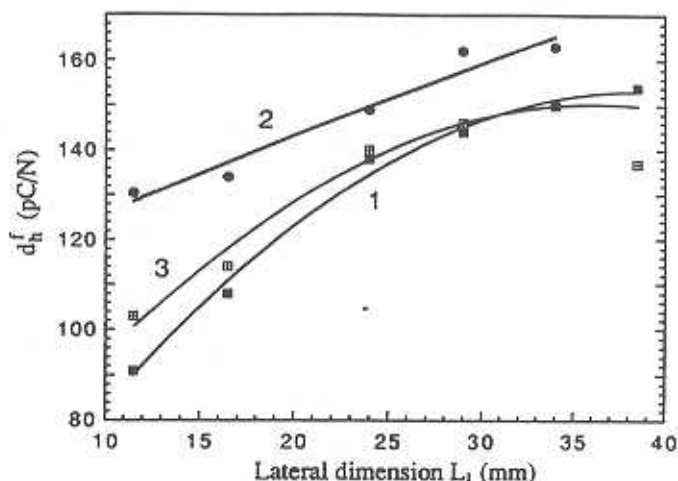


FIGURE 2 The hydrostatic charge coefficient of composite I (Spurs epoxy matrix) as a function of the sample lateral dimension L_1 . Curve 1 is for the composite without edge strips, curve 2 is for the composite with alumina edge strips, and curve 3 is for the composite with GRP edge strips. Solid lines are drawn to guide eyes.

one repeating unit of a large 2-2 composite. Because of the non-uniform strain profile in the lateral directions, d'_{31} should be calculated using the relation $d'_{31} = \bar{S}_1/E_3$ where \bar{S}_1 is the averaged strain in the 1-direction and E_3 is the applied electric field in the 3-direction. The results are plotted in Figure 3(b). For the composite without face plates, $d_{31} = -128$ pC/V. Evidently, the value of d_{31} is greatly reduced by the face plates especially when t/L_1 is small. As L_1 decreases, the clamping effect of face plates becomes less effective which leads to the rapid increases of d'_{31} .

In practice, a face plated 1-3 composite may not reach the limit $t/L \rightarrow 0$ for which d'_h reaches maximum. Therefore, it is useful to know how much d'_h of a face plated 1-3 composite is off from its limiting value. From our earlier work on 2-2 composites,¹⁰ it can be shown that both d_h and d_{31} follow approximately a linear relationship with t/L . Indeed, the data here, when plotted against t/L_1 , fall on a straight line, as shown in Figure 4. Hence, the limiting value of d'_h and d'_{31} can be extrapolated from the figure. For this composite structure, in the $t/L_1 \rightarrow 0$ limit, d'_h should reach 180 pC/N and $d'_{31} = 15.5$ pC/N. Since this d'_h value is for the sample with $L_2 = 27$ mm, in the limit of both t/L_1 and $t/L_2 \rightarrow 0$, d'_h should be above 200 pC/N. For the sample investigated, at $L_1 = 38.5$ mm and $L_2 = 27$ mm d'_h value is 160 pC/N, which is already about 80% of the limiting value.

To improve the clamping effect of the face plates on 1-3 composites, edge strips were added on this face plated composite. Shown in Figure 5 are the comparison of strain profiles of the sample of $t/L_1 = 0.196$ with and without edge strips. Two different edge strips were used here, one is GRP plate (thickness = 1.6 mm) and the other is alumina plate (thickness = 3.5 mm). It is evident that the edge strips improve the uniformity of the strain profiles. For the alumina plates, the measured d_{31} value is -18.5 pC/N, which is very close to the limiting value of d'_{31} at $t/L_1 \rightarrow 0$. However, the effect of GRP plates is much smaller due to its relatively lower elastic stiffness and small thickness.

The comparison of the hydrostatic charge coefficient d_h between the three config-

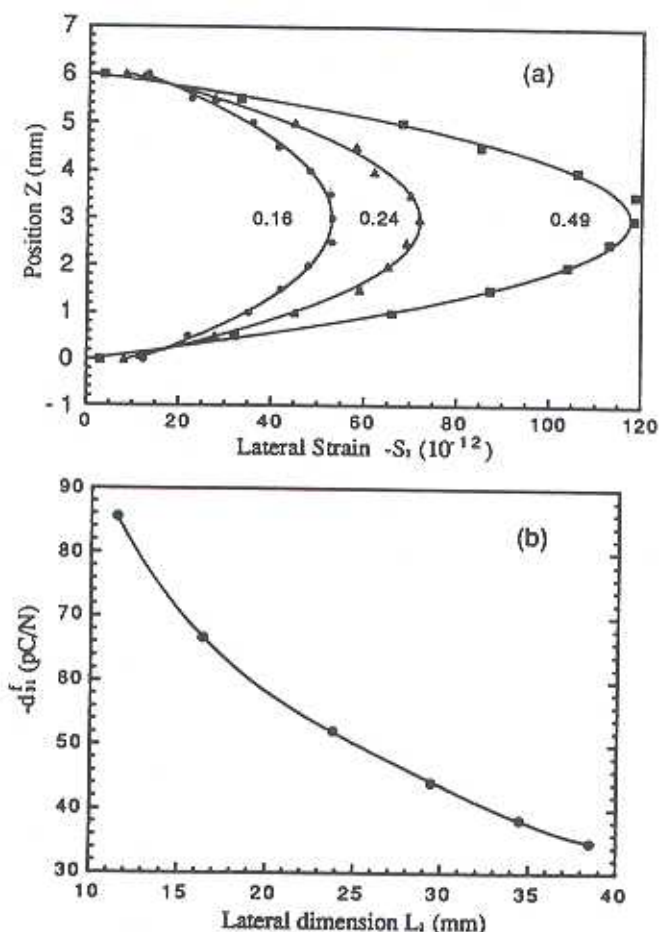


FIGURE 3 (a) The lateral strain S_1 profile of the composite I under 1 V/m driving electric field for different t/L_1 ratio. The label for each curve is the ratio t/L_1 . The incomplete clamping of the face plates on 1-3 composite is reflected by the non-uniform strain profile of S_1 , (b) the dependence of d'_{31} on the sample lateral dimension L_1 .

urations (without edge strips, with GRP edge strips, and with alumina edge strips) is shown in Figure 2. The effect of GRP edge strips is not significant. When an edge strip is used in face plated composite structure, it will influence the composite response in two opposite ways. On one hand, it reduces d_{31} for samples with finite t/L , hence enhances d_h . On the other hand, it will clamp the composite in the 3-direction in the region near it, which leads to the reductions of d_{33} and d_h . This latter effect is illustrated in Figure 6 where the surface profiles in the ceramic poling direction (the 3-direction) for face plated composite with and without edge strips are compared. The interface between the edge strip and the face plated composite is located at $x = 0$. Due to the cancellation of the two competing effects, the GRP edge strips do not change d_h very much as has been shown in Figure 2. In the limit of $t/L \rightarrow 0$, the three configurations should yield the same d_h . That is, as far as the hydrostatic response is concerned, the edge strips do not make much difference when t/L is very small. However, the edge strips do have the effect of reducing shear stress

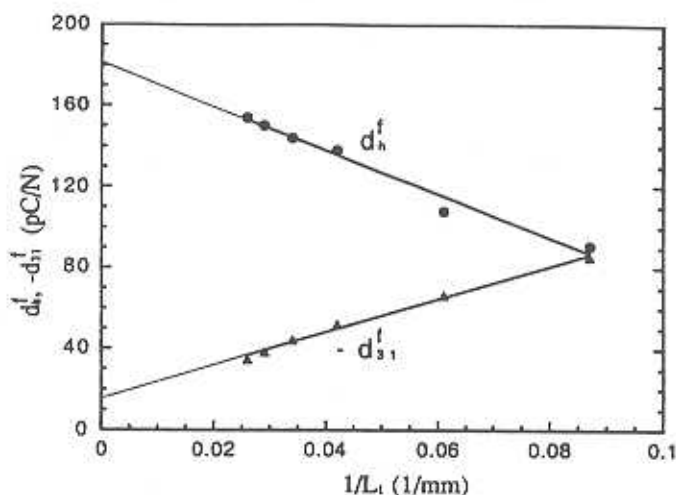


FIGURE 4 The linear relationship between d_n^f , d_{31}^f , and $1/L_1$.

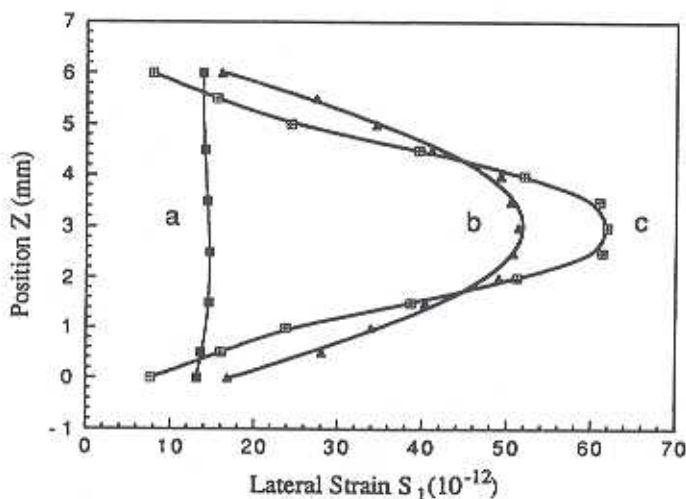


FIGURE 5 The comparison of the strain profile S_1 for the face plated composite I at $1/L_1 = 0.196$. Curve *a* is for the composite with alumina edge strips, curve *b* is for the composite with GRP edge strips, and curve *c* is the one without edge strips. The composites were driven under 1 V/m electric field.

concentration at the side boundaries of the face plate-1-3 composite interface, which improve the mechanical integrity of the composite structure.

IV. EXPERIMENTAL RESULTS FOR COMPOSITE II.

The polymer matrix of polyurethane mixed with microballon has much smaller Young's modulus and Poisson's ratio compared with Spurr's epoxy as listed in Table I. Without face plates, the composite II has a d_n of 45 pC/N and a d_{31} of -130 pC/N. Although softer polymer matrix reduces the polymer self-loading, the much re-

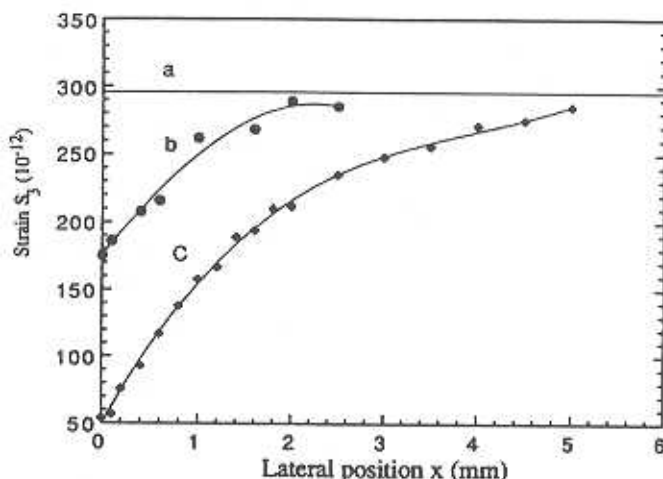


FIGURE 6 The effect of edge strips on the longitudinal strain S_3 . For the comparison, S_3 for the composite without edge strips is shown in curve *a*. Curve *b* is for the composite with GRP edge strips and curve *c* is for the alumina edge strips. The interface between the face plated composite and edge strip is at $x = 0$.

duced shear modulus of the polymer matrix also reduces the stress transfer between the polymer matrix and ceramic rods resulting in a small d_h . With GRP face plates, d_h value is increased significantly as shown in Figure 7(a). Similar to the composite I, d'_{31} also exhibits a strong t/L_1 dependence. The dimensional dependence of d'_{31} was also measured and is plotted in Figure 7(b). Though d'_{31} value here is comparable to those of composite I, d'_h is clearly much higher for the composite with a soft polymer matrix. As will be shown later in the paper, this increase is due to the reduction in the polymer matrix self-loading which produces a higher effective stress level in the ceramic rods.

The influence of 3.5 mm thick alumina edge strips on the hydrostatic response of this face plated composite is also shown in Figure 7(a). The improvement of the edge strips on this face plated composite is only about 10% at most. This is the result of edge strip clamping on d_{33} response of the composite since with a soft polymer matrix, the elastic stiffness in the 3-direction is much smaller than that of the edge strips and the effect of clamping in the 3-direction will be more severe in composite II.

For composite II, the plots of d'_h and d'_{31} as a function of t/L_1 did not fall on a straight line. It was also found that the dielectric constant and piezoelectric constant d'_{33} of the sample decreased as the sample dimension L_1 decreases. All these are quite different from the results of composite I. Careful inspection on composite II reveals that some PZT rods in the composite were broken when the sample was recycled during the hydrostatic measurement and during the cutting process to reduce L_1 . To correct this, the dielectric constant ϵ of individual PZT rods was measured and the data is used to calculate the percentage α of the broken rods in the samples by assuming the sample dielectric constant do not depend on the sample lateral dimensions if no ceramic rod is broken in the sample. Using this method, the measured d'_{33} , d'_h and d'_{31} were corrected by dividing them by the factor of $(1 - \alpha)$ at the corresponding L_1 value. After this correction, d'_{33} becomes almost independent

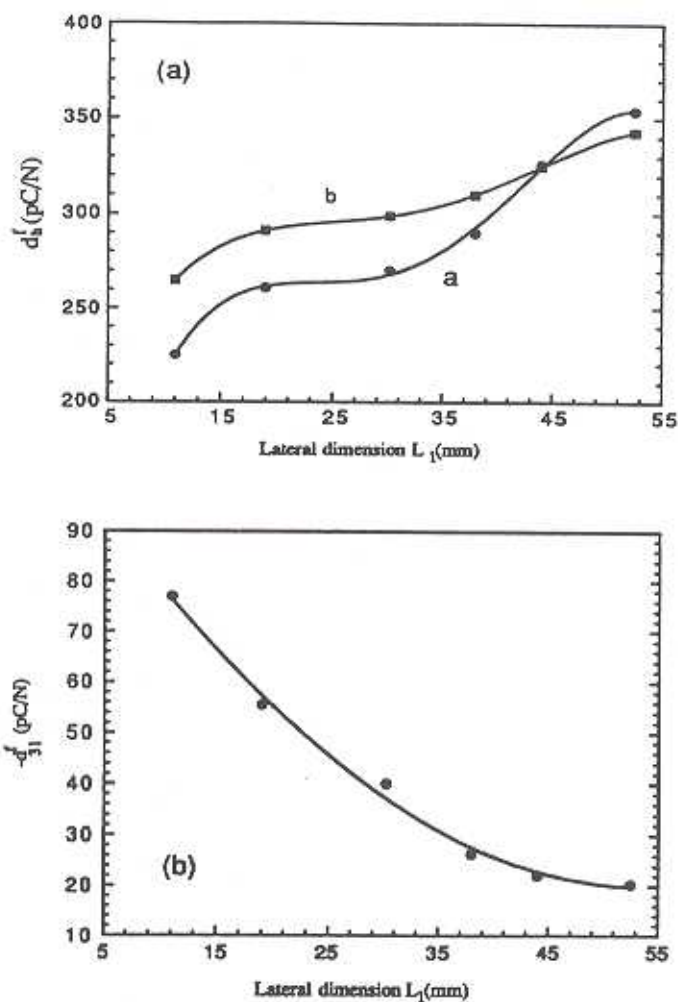


FIGURE 7 (a) The dependence of d_h^f on the sample lateral dimension L_1 for the composite II. Curve *a* is for the composite without edge strips and curve *b* is that with alumina edge strips. (b) The dependence of d_{31}^f on the sample lateral dimension L_1 for the composite II.

of the sample lateral dimension as we have expected. The results after the correction for d_h^f and d_{31}^f are plotted in Figure 8 and indeed, the data follow a linear relationship with $1/L_1$. From the linear extrapolation, the limiting values of d_h^f and d_{31}^f at $1/L_1 \rightarrow 0$ are obtained and they are 440 pC/N and -6.6 pC/N respectively. Therefore, the hydrostatic figure of merit for this configuration can be as high as $50,600 \cdot 10^{-15} \text{ m}^2/\text{N}$.

In Table III, the values of d_h , d_{31} , d_h^f , d_{31}^f , measured at smallest t/L_1 ratio, and the values of d_h^f , d_{31}^f at $t/L_1 \rightarrow 0$, as well as the hydrostatic figure of merit for the two composites are listed. Needless to say, the exceptionally high $d_h g_h$, high d_h , light weight, and relative easiness of manufacturing face plated 1-3 composites make them superior compared with currently available hydrophone designs.

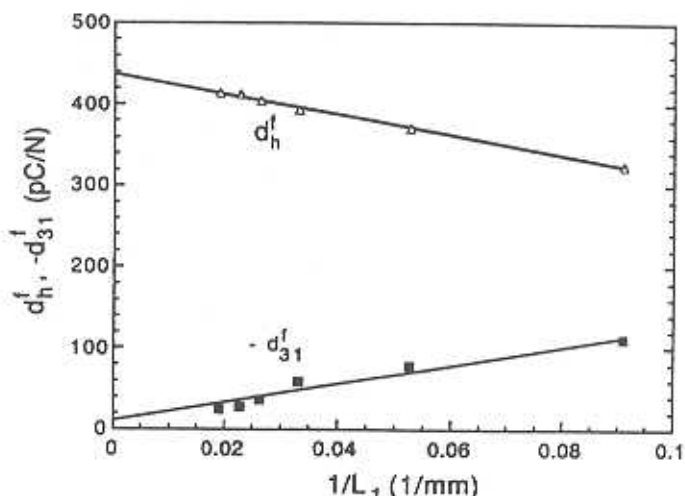


FIGURE 8 The modified d_h^f and d_{31}^f (corrected for the broken rods in the composite) as a function of $1/L_1$.

TABLE III
Summary of the properties of the two composites

	d_{31} (pC/N)	d_h	d_{31}^f	d_h^f	d_{31}^f (limit)	d_h^f (limit)	$d_h^f g_h^f$ (limit) (m^2/N)
Composite I	-128	43	-34.8	154	-17	181	7378 (10^{-15})
Composite II	-130	45	-23.9	414	-6.6	438	50,600 (10^{-15})

* d_{31} and d_h are for 1-3 composite without face plates, d_{31}^f and d_h^f are for 1-3 composites with face plates at their initial dimension. d_{31}^f (limit) and d_h^f (limit) are taken from figures 4 and 8.

V. THEORETICAL TREATMENT OF CLAMPING EFFECT OF FACE PLATES ON 1-3 COMPOSITES

From the experimental results in the sections III and IV, it is clear that in order to have a high hydrostatic response of a face plated 1-3 composite, a polymer matrix with a low Young's modulus is preferred. On the other hand, a 1-3 composite made of soft polymer matrix such as foamed polyurethane used here has the problem of low mechanical integrity, which may result in failure of a device. In practice, one has to balance these two effects. In this section, we will present a theoretical treatment which relates various design parameters to the hydrostatic response of a face plated 1-3 composite.

Clamping effect of stiff face plates on a soft piezoelectric material has been analyzed by Wang *et al.*

$$d'_{31} = d'_{32} = \frac{\overline{d}_{31}}{1 + \frac{2(\overline{s}_{11} + \overline{s}_{12})}{\gamma(s_{11}^b + s_{12}^b)}} \quad (1)$$

$$d'_{33} = \overline{d}_{33} + \frac{\overline{s}_{13}(d'_{31} + d'_{32} - 2\overline{d}_{31})}{\overline{s}_{11} + \overline{s}_{12}} \quad (2)$$

$$d'_h = \overline{d}_{33} + \overline{d}_{31} \frac{2\gamma(s_{11}^b + s_{12}^b) - 4\overline{s}_{31}}{\gamma(s_{11}^b + s_{12}^b) + 2(\overline{s}_{11} + \overline{s}_{12})} \quad (3)$$

where the quantities on the left hand side of the equations are those for the face plated samples. The quantities with a bar on the top (such as \overline{d}_{31}) on the right hand side of the equations are those for the soft piezoelectric material and the superscript *b* refers to the face plate. $\gamma = t/t^b$ is the thickness ratio of the piezoelectric material to the face plate. Equations (1), (2), and (3) are derived under the condition that the lateral strains in the face plate and the soft piezoelectric material are equal, a situation corresponds to $t/L \rightarrow 0$ limit here.

To use these equations for the face plated 1-3 composite, the effective material properties have to be evaluated. Though the behavior of composites without face plates can be quite different from that calculated based on the isostrain model, it is shown that the difference of the strain profile between the polymer and ceramic rods in the 3-direction becomes very small for composites with thick face plates, and the composite can be treated using the isostrain model.⁸

The basic assumption for the isostrain model used here is that the strains in both the polymer and ceramic rods in the 3-direction are equal while the stresses in the 1- and 2-directions in the two constituents are the same. Based on these assumptions, it can be derived

$$\overline{D}_{33} = \frac{\overline{D}_3}{T_3} = \frac{V^c s_{33}^c d_{33}^c}{V^c s_{33}^c + (1 - V^c) s_{33}^p} \quad (4)$$

$$\overline{s}_{33} = \frac{\overline{S}_3}{T_3} = \frac{s_{33}^p d_{33}^c}{V^c s_{33}^c + (1 - V^c) s_{33}^p} \quad (5)$$

where the superscripts *p* and *c* refer to the polymer and ceramic, respectively.

Assuming the sample is subjected to a stress T_1 in 1 or 2 direction, from the constitutive relations and isostress assumption, one can get

$$S_3^c = s_{33}^c T_3^c + s_{13}^c T_1 \quad (6)$$

$$S_1^c = s_{11}^c T_1 + s_{13}^c T_3^c \quad (7)$$

$$S_2^c = s_{12}^c T_1 + s_{23}^c T_3^c \quad (8)$$

For the polymer phase, similar equations can be obtained by simply replacing superscript *c* by *p*. Furthermore,

$$V^c T_3^c + (1 - V^c) T_3^p = 0 \quad (9)$$

$$\overline{D}_3 = d_{33}^c T_3^c V^c + d_{31}^c T_1 V^c \quad (10)$$

$$\overline{S}_2 = V^c S_2^c + (1 - V^c) S_2^p \quad (11)$$

$$\bar{S}_1 = V^c S_1^c + (1 - V^c) S_1^p \quad (12)$$

Solving these equations yields:

$$\frac{\bar{S}_3}{T_1} = \frac{\bar{S}_3}{T_1} = \frac{s_{33}^c s_{13}^p (1 - V^c) + V^c s_{13}^c s_{33}^p}{V^c s_{33}^c + s_{33}^p (1 - V^c)} \quad (13)$$

$$\bar{s}_{11} = (1 - V^c)[s_{12}^p + s_{13}^p(s_{13}^p - s_{13}^c)V^c c_a] + V^c[s_{12}^c - s_{13}^c(s_{13}^p - s_{13}^c)(1 - V^c)c_a] \quad (14)$$

$$\bar{s}_{12} = (1 - V^c)[s_{12}^p + s_{13}^p(s_{13}^p - s_{13}^c)V^c c_a] + V^c[s_{12}^c - s_{13}^c(s_{13}^p - s_{13}^c)(1 - V^c)c_a] \quad (15)$$

$$\bar{d}_{31} = d_{33} V^c c_a [s_{13}^p (s_{13}^p - s_{13}^c) (1 - V^c)] + d_{31} V^c \quad (16)$$

where $c_a = 1/((1 - V^c)s_{33}^c + s_{33}^p V^c)$. From these relations, d_h^c and d_{31}^c are calculated for the two composite structures investigated. Some of the material parameters used for the calculations have been listed in Tables I and II and the elastic compliance data for PZT-5H are used for the ceramic rods.¹⁴ ($\gamma = 7.1$ for spurrs epoxy composite and $\gamma = 3.46$ for polyurethane composite). The calculated results for the composite with Spurrs epoxy matrix (composite I) are, $d_h^c = 171$ pC/N and $d_{31}^c = -17.6$ pC/N; and for the composite with foamed polymer matrix (composite II), $d_h^c = 480$ PC/N and $d_{31}^c = -0.2$ PC/N. These values are in very good agreement with the experimental data when extrapolated to t/L_1 and $t/L_2 \rightarrow 0$ limit. It indicates that the theoretical results here provide quite accurate prediction on the hydrostatic response of a face plated 1-3 composite.

From the above equations, the relationship between the hydrostatic response of a face plated 1-3 composite and s_{11}^p and σ of the polymer can be derived:

$$d_h^c = d_{33} s_{11}^p V^c c_a + [V^c d_{31} - V^c (1 - V^c) d_{33} c_a (s_{13}^p + \sigma s_{11}^p)] \quad (17)$$

$$\left\{ \frac{2\gamma(s_{11}^p + s_{12}^p) - 4c_a[V^c s_{11}^p s_{13}^p - s_{33}^c \sigma s_{11}^p (1 - V^c)]}{\gamma(s_{11}^p + s_{12}^p) + 2[V^c (s_{11}^p + s_{12}^p) + (1 - V^c) s_{11}^p (1 - \sigma) - 2V^c c_a (1 - V^c) (s_{13}^p + \sigma s_{11}^p)^2]} \right\}$$

Figure 9(a) shows the dependence of d_h^c on s_{11}^p for three different Poisson's ratio of the polymer matrix: $\sigma = 0.15, 0.3$, and 0.4 . GRP is used here as face plates. The ceramic used in the calculation is PZT-5H.¹⁴ The ceramic rods content of 15% and a γ of 3.5 are used in the calculation. From Figure 9(a), it is clear that the effect of the Poisson's ratio of the polymer phase on d_h^c depends critically on the elastic compliance of the polymer. When the elastic compliance of the polymer matrix is below, for example, 5×10^{-8} , there is little change in d_h^c when the Poisson's ratio is increased from 0.15 to 0.4. However, a drastic decrease of d_h^c with σ occurs for polymers with smaller elastic compliance. Furthermore, there is not much decrease in d_h^c when s_{11}^p is reduced from 5×10^{-8} (close to the value of the foamed polyurethane used for the composite II) to 5×10^{-9} , a polymer ten times harder than the polymer matrix used for the composite II. With an elastically stiffer polymer matrix, the mechanical integrity of the device is improved significantly while there is not much loss in the hydrostatic response. This illustrates that for a composite with a polymer matrix ten times stiffer than the polymer matrix for the composite II, there is little reduction in the hydrostatic figure of merit while there is a substantial increase in its mechanical integrity. Apparently, Spurrs epoxy is not a suitable choice either for the polymer matrix for the face plated 1-3 composite discussed here.

Figure 9(b) shows the dependence of d_h^c on s_{11}^p , with different ratio γ (thickness ratio of 1-3 composite to the face plate) with $\sigma = 0.3$ for the polymer matrix, which should

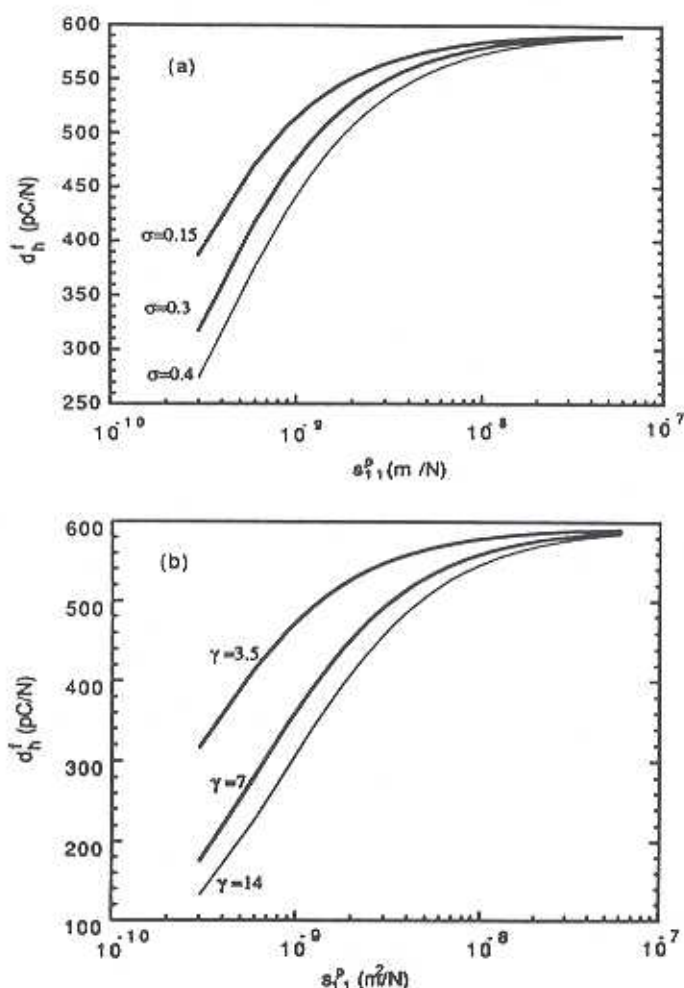


FIGURE 9 (a) The dependence of d_h^i of a face plated 1-3 composite, which has 15% PZT 5H rod content and GRP face plates with $\gamma = 3.5$, on the compliance s_{11} of the polymer matrix. Three Poisson's ratios are used: $\sigma = 0.15, 0.3$, and 0.4 as labeled on the figure. The curves are calculated using Equation (17). (b) The dependence of d_h^i of a face plated 1-3 composite, which has 15% PZT 5H rod content and GRP face plates, on the compliance s_{11} of the polymer matrix for different γ (the thickness ratio of the face plate t_f and the 1-3 composite t).

provide valuable information on the selection of face plate thickness in reference with the thickness of 1-3 composite.

VI. SUMMARY

The hydrostatic response of a 1-3 composite can be significantly increased by using face plates to (1) improve the stress transfer in the 3-direction; (2) reduce the Poisson's ratio effect and d_{31} effect; (3) improve the mechanical integrity of the composite structure. In this paper, we show that for a face plated 1-3 composite with a soft

polymer matrix and 15% ceramic rod content, its hydrostatic figure of merit $d_h g_h$ can reach more than $50,000 \times 10^{-15}$ (m^2/N). However, due to the nature of the shear coupling between the face plates and 1-3 composite, the hydrostatic response of a face plated 1-3 composite will depend on the sample lateral dimensions. The hydrostatic response will increase as the ratio of the thickness to the lateral dimension (t/L) becomes small, for a large t/L ratio, improvement of the hydrostatic response due to the face plates is not significant. One possible method to increase d_h for samples with a large t/L ratio is to use edge strips. However, the study here shows that the effect is not significant due to the two opposite roles an edge strip plays on a face plated 1-3 composite. Therefore, the key to increase hydrostatic response is to use small t/L ratio for a face plated 1-3 composite.

To balance the requirement of high hydrostatic sensitivity and mechanical integrity, a proper polymer matrix with the right elastic properties should be used. In the paper, we showed that the two face plated composites tested represent the two extreme cases with the Spurr's epoxy matrix on the hard side and the polyurethane with 50% microballon on the soft side of the polymer matrix spectrum. A polymer matrix with its elastic properties in between the two would be a good choice to balance the two requirements as mentioned previously. In general, the theoretical results presented here can provide a useful guideline for the optimum design of face plated 1-3 composites.

ACKNOWLEDGMENTS

The authors wish to thank Fiber Materials, Inc. for providing the 1-3 composite with polyurethane matrix (the composite II). The authors also wish to thank Dr. W. Smith and Dr. W. Reader for many stimulating discussions. This work was supported by the Office of Naval Research.

REFERENCES

1. R. E. Newnham, D. P. Skinner and L. E. Cross, *Mat. Res. Bull.*, **13**, 525 (1978).
2. K. A. Klicker, Ph.D. Thesis, The Pennsylvania State University, 1980.
3. T. R. Gururaja, Ph.D. Thesis, The Pennsylvania State University, 1984.
4. W. A. Smith and B. A. Auld, *IEEE Trans. UFFC*, **38**, 40 (1991).
5. M. J. Haun and R. E. Newnham, *Ferroelectrics*, **68**, 123 (1986).
6. Wenwu Cao, Q. M. Zhang and L. E. Cross, *J. Appl. Phys.*, **72**, 5814 (1992).
7. Q. M. Zhang, Wenwu Cao, H. Wang and L. E. Cross, Proc. IEEE ISAF8 252, 1992.
8. Wenwu Cao, Q. M. Zhang, J. Zhao and L. E. Cross, preprint and to be published.
9. H. Wang, Q. M. Zhang, L. E. Cross and A. O. Sykes, submitted to *Ferroelectrics* (1993).
10. Q. M. Zhang, Wenwu Cao, J. Zhao and L. E. Cross, submitted to *IEEE Trans. UFFC* (1993).
11. C. G. Oakley, Ph.D. Thesis, The Pennsylvania State University, 1991.
12. CRC Handbook of Chemistry and Physics, CRC Press, Inc., 1980-1981.
13. Q. M. Zhang, S. J. Jang and L. E. Cross, *J. Appl. Phys.*, **65**, 2808 (1989).
14. PZT-5H is the trade mark of Morgan Matric Inc., Veritron Div. for its La doped PZT. From the data sheet, $d_{33} = 593$ (pC/N), $d_{31} = -275$, $s_{11} = 1.65 \times 10^{-11}$ (m^2/N), $s_{12} = -0.478 \times 10^{-11}$, $s_{33} = 2.08 \times 10^{-11}$, $s_{13} = -0.845 \times 10^{-11}$.